# Covalent Assembly of Stilbene-Based Monolayers: Factors Controlling Molecular Interactions

**Atindra D. Shukla,[†] David Strawser,[†] Andre C. B. Lucassen,[†] Dalia Freeman,[†] Hagai Cohen,[‡] D. Amilan Jose,[§] Amitava Das,[§] Guennadi Evmenenko,[||] Pulak Dutta,[||] and Milko E. van der Boom*,[†]**

*Department of Organic Chemistry, Department of Chemical Research Support, The Weizmann Institute of Science, Rehovot 76100, Israel, Central Salt and Marine Chemicals Research Institute, Gujarat, India, and Department of Physics and Astronomy, and Materials Research Center, Northwestern University, Evanston, Illinois 60208-3113*

*Received: June 17, 2004; In Final Form: August 18, 2004*

A new series of stilbene-based chromophores have been used to prepare structurally related siloxane-based monolayers in order to determine which factors control the intermolecular chromophore−chromophore interactions in the solid state. The reaction of chromophore precursors 4-styrylpyridine (**1**), 4-[2-(4-bromophenyl)-vinyl]-pyridine (**2**), 4-(2-naphthalen-1-ylvinyl)-pyridine (**3**), 4-(2-anthracen-9-ylvinyl)-pyridine (**4**), and 4-(2-pyren-2-ylvinyl)-pyridine (**5**) with excess 3-iodo-*n*-propyl-1-trimethoxysilane resulted in the corresponding salts **6**−**10** in quantitative yield. The assembly of chromophores **6**−**10** on hydrophilic substrates from solution resulted in the formation of densely packed monolayers with a film thickness of ∼1 nm. The average chromophore density (∼1 chromophore/50 Å$^2$) is well within the range that allows $\pi-\pi$ stacking to occur. Transmission UV−vis spectroscopy of the siloxane-based films shows that the intermolecular interactions are a function of the aryl groups (e.g., phenyl, bromophenyl, naphthalene, anthracene, and pyrene). Relatively weak electronic interactions occur between the surface-bound chromophores **6**, **7**, and **10**, whereas strong electronic interactions occur between surface-bound chromophores **8** and **9**. The series of monolayers on sodium lime glass and polished silicon is characterized by a combination of physicochemical methods including X-ray photoelectron spectroscopy, advancing aqueous contact angle measurements, optical spectroscopy, atomic force microscopy, and synchrotron X-ray reflectivity.

## Introduction

The transfer of molecular properties into macroscopic phenomena is a key step in the formation of many functional organic materials. Chromophore aggregation has been identified as one of the most important problems to be addressed in the formation of device-quality organic materials for electro-optical applications.[1−3] Chromophore−chromophore interactions are known to limit the maximum possible nonlinear optical and electro-optical responses in poled polymers and other systems. The use of bulky substituents or specially designed dendritic polymers prevents chromophore aggregation and enhances the maximum possible electro-optical responses in poled polymers.[1−3] On the other hand, molecular interactions are crucial for the development of organic field effect transistors (OFETs).[4−6] Intermolecular chromophore interactions in solution and in the solid state have been studied extensively by Würthner,[7,8] Dalton,[1,2,9] Blanchard,[10,11] Pagani,[12−14] and many others.[3,12,15−26] This issue has also been addressed in several theoretical investigations.[27−30] Various studies have been reported on parallel (H-aggregate) or inclined (J-aggregate) dipole−dipole arrangements in Langmuir−Blodgett (LB) films which give rise to spectral changes (hypsochromic or bathochromic shifts).[12,22−26] Nevertheless, there are still fundamental gaps in the understanding of the influence of chromophore design on material structure−function relationships. One challenge is apparent: For a given chromophore, which structural parameters can be tuned to efficiently transfer the desired molecular properties into a thin film? For instance, it is known that various trialkoxysilane and trichlorosilane functionalized stilbene- and azobenzene-based chromophores form intrinsically acentric monolayers and multilayers on hydrophilic substrate surfaces.[31−41] These siloxane-based materials exhibit excellent nonlinear optical and electro-optical responses and have been successfully integrated into various all-organic device-type structures (e.g., modulators, switches, waveguides).[42−45] The absence of significant hypsochromic shifts in these densely packed films argues against centrosymmetric H-type chromophore aggregation, which is known sometimes to suppress the second-order nonlinear optical responses in LB systems.[12] Kinetic studies of the self-assembly of stilbene- and azobenzene-based monolayers did not reveal the reason behind the absence of chromophore aggregates at high chromophore densities.[46,47] In the present study, a representative series of stilbene-based monolayers was used to investigate the structural factors which control structure−property relationships in these systems.

## Results and Discussion

The reaction of the known chromophore precursors 4-styrylpyridine (**1**),[48] 4-(2-(4-bromophenyl)-vinyl)-pyridine (**2**),[49] 4-(2-naphthalen-1-ylvinyl)-pyridine (**3**),[50] 4-(2-anthracen-9-ylvinyl)-

* To whom correspondence should be addressed. E-mail: milko.vanderboom@weizmann.ac.il.
[†] Department of Organic Chemistry.
[‡] Department of Chemical Research Support.
[§] Central Salt and Marine Chemicals Research Institute.
[||] Department of Physics and Astronomy, and Materials Research Center.

10.1021/jp047358s CCC: $27.50 
Published on Web 10/19/2004

**TABLE 1: Long-Wavelength UV−vis Absorption Maxima ($\lambda_{max}$) of Chromophores 1−10 in THF and of the Chromophore Monolayers 6−10 on Glass Substrates**

| chromophore | $\lambda_{max}$ (nm) | chromophore | $\lambda_{max}$ (nm) | $\Delta\lambda_{max}$[a] (nm) |
|---|---|---|---|---|
| **1** | 307 | **6** | 350 | +43 |
| **2** | 312 | **7** | 353 | +41 |
| **3** | 329 | **8** | 368 | +39 |
| **4** | 370 | **9** | 442 | +72 |
| **5** | 376 | **10** | 447 | +71 |

| SAM | $\lambda_{max}$ (nm) | $\Delta\lambda_{max}$[b] (nm) |
|---|---|---|
| **6** | 344 | −6 |
| **7** | 352 | −1 |
| **8** | 388 | +20 |
| **9** | 457 | +15 |
| **10** | 455 | +8 |

[a] $\lambda_{max}$(chromophores **6**−**10**) − $\lambda_{max}$(chromophores **1**−**5**). [b] $\lambda_{max}$(SAMs **6**−**10**) − $\lambda_{max}$(chromophores **6**−**10**).

pyridine (**4**),[51] and 4-(2-pyren-2-ylvinyl)-pyridine (**5**)[50] with an 8-fold excess of 3-iodo-*n*-propyl-1-trimethoxysilane in dry THF under $N_2$ at 80 °C in a pressure vessel resulted in the corresponding salts **6**−**10** in quantitative yield (eq 1)

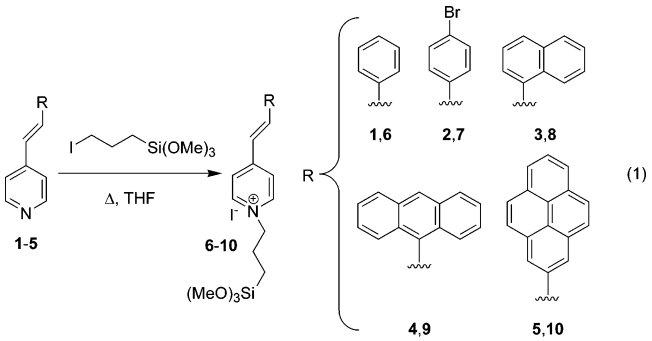


The relatively low solubility of the new chromophores in common hydrocarbon solvents facilitated their isolation by washing with cold pentane (−25°C) to extract excess starting material. All compounds (**6**−**10**) have been characterized by $^1H$ and $^{13}C\{^1H\}$ NMR and UV−vis measurements. For instance, the $^1H$ and $^{13}C\{^1H\}$ NMR spectra of compound **6** exhibit a characteristic triplet resonance at $\delta = 4.47$ ppm and a signal at $\delta = 62.21$ ppm, respectively, for the $N-CH_2$ moiety. The optical spectra of pyridinium-based salts **6**−**10** exhibit large characteristic bathochromic shifts (39−72 nm) of the charge-transfer band versus those of the chromophore precursors **1**−**5** (Table 1).

Freshly cleaned float glass and silicon substrates were treated with a dry THF solution of **6**−**10** (1 mM) at 70 °C for 24 h in a sealed vessel under $N_2$ with the exclusion of light. The solution was allowed to cool to room temperature, and the colored substrates were rinsed repeatedly with dry THF, acetone, and 2-propanol with sonication and dried under a stream of $N_2$. The new self-assembled monolayers (SAMs) adhere strongly to the hydrophilic substrates, demonstrated by insolubility in common organic solvents and the inability to be removed from the substrate by Scotch tape. The functionalized substrates were stored in a glovebox under $N_2$ in the dark at room temperature. The new monolayers have been characterized by a full complement of physicochemical techniques: optical (UV−vis) spectroscopy, advancing contact angle (CA) measurements, X-ray photoelectron spectroscopy (XPS), synchrotron X-ray reflectivity (XRR), and atomic force microscopy (AFM).

Significant optical (UV−vis) differences were found between films of chromophores **8**−**9** and the corresponding chromophores in solution, whereas relatively minor differences were observed between films of chromophores **6**, **7**, **10** and the corresponding chromophores in solution (Figure 1). Table 1 displays the UV−vis data of **6**−**10** in solution and as SAMs. The following trend for $\Delta\lambda_{max}$ is apparent: phenyl (**6**) < Br−phenyl (**7**) < pyrene (**10**) < anthracene (**9**) < naphthalene (**8**).

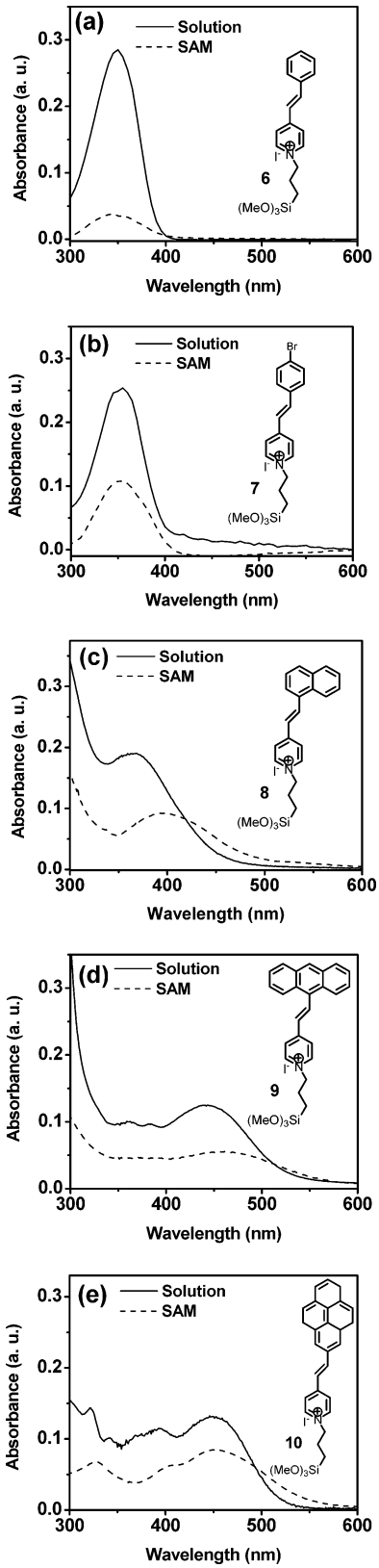


**Figure 1.** Optical absorption (UV−vis) measurements of compounds **6**−**10** in dry THF and SAMs **6**−**10** on glass.

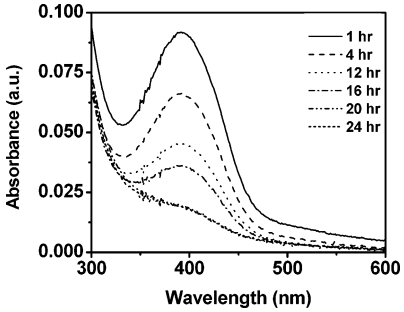


**Figure 2.** Optical absorption (UV−vis) measurements of SAM **8** on glass in air and light at different time intervals.

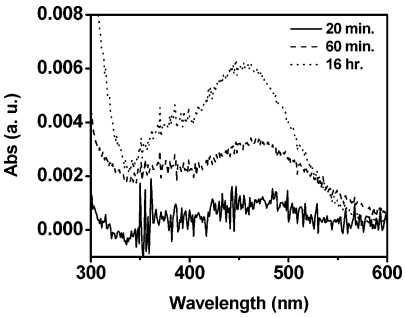


**Figure 3.** Representative optical absorption (UV−vis) data at three different time intervals for the formation of a **9**-based chromophore monolayer on clean glass from a THF solution (1 mM, 60 °C).

Large shifts in $\lambda_{max}$ toward lower energy for the fused ring systems **8**−**10** compared to **6** and **7** are believed to be due to the lowering of the energy for the LUMO. Further, the large difference in $\Delta\lambda_{max}$ (e.g., 20 nm for **8**, 15 nm for **9**) is presumably caused by the electronic coupling of the respective chromophores **8**−**9**. N-alkylation in **8**−**10** is expected to bring down the LUMO further and thus supports the observed shift to a longer wavelength. According to the exciton theory, stronger electronic coupling produces a larger red shift.[52,53] Thus, it appears that the electron coupling is stronger than repulsive interactions that might occur between the positively charged pyridinium moieties.

Photobleached samples of the films of **8** were obtained after exposure to visible light for 24 h in air as shown in Figure 2. Materials exhibiting photobleachable UV−vis absorption bands may have applications in optical data storage.[14]

Several routes are believed to be operative in the assembly of thiol- and siloxane-based monolayers. Two commonly observed pathways are the island- and uniform-type film growths of the system.[54−60] We observed recently that the solution deposition of a trimethoxysilane functionalized azobenzene-based chromophore onto hydrophilic silicon oxide surfaces may proceed via a uniform growth mechanism.[47] Monolayer formation on transparent substrates (e.g., glass, quartz) is readily monitored by optical (UV−vis) spectroscopy because of the large extinction coefficients. Film formation with chromophore **9** was quenched at measured time intervals ($t$ = 20 min, 1 h, and 16 h). The samples were washed immediately with an excess of dry toluene and THF and sonicated in acetone for 2 min. A representative plot of the absorption bands of chromophore **9** versus the deposition time is displayed in Figure 3 and clearly illustrates that large shifts ($\Delta\lambda_{max(solv-film)} > 15$ nm) occur in the optical absorption maximum at the initial stages of film formation. No further significant shifts in the HOMO−LUMO charge transfer (CT) optical absorption are observed by ex situ monitoring of film growth formation.

UV−vis measurements reveal the formation of chromophore aggregates at high molecular densities for films of **8**−**10** (Figure 1, Table 1). The presence of molecular aggregates on the surface, even in the early stages of the interrupted growth process as exemplified in Figure 3 for film **9**, indicates that the intramolecular interactions are not sterically enforced in the fully formed films by close packing of the chromophores. Moreover, the microstructure of the fully formed monolayers might be directed by the interchromophore interactions during the initial stage of the assembly process. The origin of the relatively weak electronic interactions in film **10** is unclear, however; it seems that structural variation of the aryl headgroup has a significant impact on the intermolecular interactions.

The advancing aqueous CA measurements of the monolayers of chromophores **6**−**10** (71° (**6**), 70° (**7**), 75° (**8**), 78° (**9**), 70° (**10**)) indicate that these films are moderately hydrophobic.

Noncontact mode AFM measurements show a uniform film formation for SAMs **6**−**10** on the silicon oxide surface of single-crystal silicon ⟨100⟩ substrates, as exemplified in Figure 4 for SAMs **7** and **10**. The stilbene-based films **6**−**10** exhibit an essentially identical surface morphology without pinholes, cracks, or grains. The SAMs **6**−**10** have a similar root-mean-square (rms) surface roughness of about 0.1 nm for $1 \times 1\ \mu m^2$ scan areas, compared to 0.06 nm for bare silicon wafers.

XPS studies were performed on **7**- and **9**-based films grown on highly doped n-type silicon. In both cases, the XPS measurements reveal the presence of the characteristic pyridinium nitrogen at 402.8 eV (SAM **7**) and 402.5 eV (SAM **9**) (Figure 5).[17,39,61] For SAMs **7** and **9**, the film thicknesses were estimated using a model for an ideal planar structure with a homogeneous film of thickness $T$

$$T \cong \lambda \sin\theta \ln(R + 1) \tag{2}$$

where $\lambda$ is the electron mean free path, $\theta$ is the takeoff angle with respect to the surface plane, and $R$ is the ratio between the intensity of the overlayer ($I_{ov}$) and the substrate ($I_{sub}$). The film thickness as derived from angle-resolved XPS (ARXPS) for SAM **7** is estimated to be 11 ± 2 Å (assuming $\lambda$ = 33 Å at the organic layer). The ARXPS data further point at a very uniform film thickness, namely a low concentration of holes or disorder in the alignment of the molecules. The thickness of film **9** is 9 ± 2 Å, in good agreement with XRR measurements (vide supra).

Specular XRR measurements were performed to gather microstructural information on films **6**−**10** (e.g., film thickness, chromophore density, and surface roughness). In general, specular XRR is determined by the electron density profile $\rho(z)$ perpendicular to the sample surface. In the Born approximation, the normalized reflectivity is

$$\frac{R(q_z)}{R_F(q_z)} = \left| \frac{1}{\rho_{Si}} \int \frac{\partial\rho(z)}{\partial z} e^{-izq_z}\, dz \right|^2 \tag{3}$$

where the wave vector transfer $|\mathbf{q}| = q_z = (4\pi/\lambda) \sin\theta$ along the surface normal, $\rho_{Si}$ is the electron density of the semi-infinite silicon substrate, $\rho(z)$ is the electron density distribution inside the film averaged over the in-plane coherence length of the X-rays (usually ∼1−3 $\mu$m), and $R_F(q_z)$ is the theoretical Fresnel reflectivity for an ideally flat substrate surface. A physically valid model for the films must be assumed in order to obtain a plausible electron density profile for each sample normal to the surface by fitting the experimental reflectivity curves while systematically varying the model parameters. For systems **6**−**10**, a model comprising a silicon substrate (with native layer of silicon oxide) and an organic layer (SAM) was used

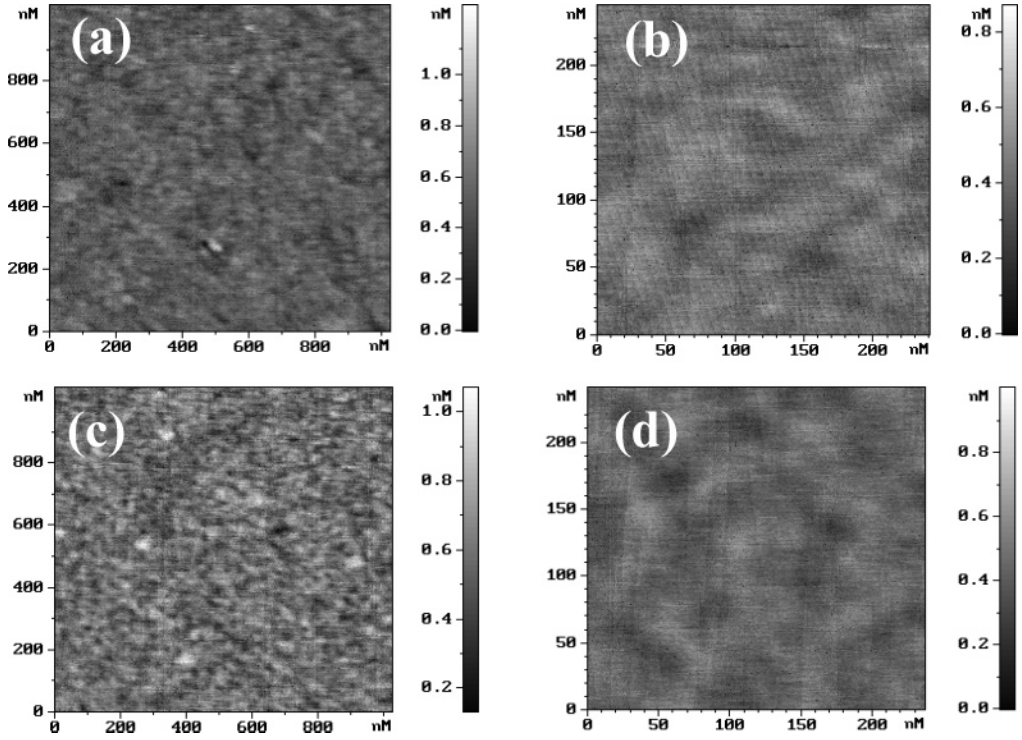


**Figure 4.** Representative AFM images at 1 × 1 and 0.25 × 0.25 $\mu$m$^2$ scan areas for SAMs **7** (parts a, b) and **10** (parts c, d).

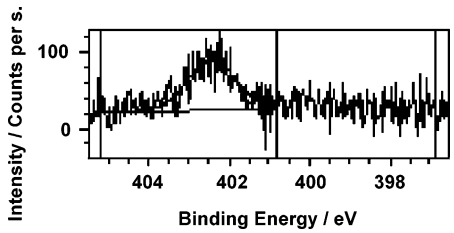


**Figure 5.** Representative XPS data for SAM **9**. XPS N (1s) spectrum showing a signal at approximately 402.5 eV, indicative of the pyridinium group.

$$\frac{R(q_z)}{R_F(q_z)} = \left| \sum_{i=0}^{N} \frac{(\rho_i - \rho_{i+1})}{\rho_{Si}} e^{-iq_z D_i} e^{-q_z^2 \sigma_{i+1}^2/2} \right|^2 \qquad (4)$$

where $N$ is the number of layers of different electron densities, $\rho_i$'s, with Gaussian broadened interfaces, $\sigma_i$'s; $\rho_{Si}$ is the electron density of the substrate, $D_i = \sum_{j=1}^{i} T_j$ is the distance from the substrate surface to the $i$th interface, and $T_j$ is the thickness of the $j$th layer. The reflectivity data were fitted to such a model, with the fitting parameters being the thickness of each layer, the electron density of each layer, and the rms width of each interface. The fits were performed using only data for which $q_z > 2q_c$ ($q_c = 0.0316$ Å$^{-1}$ for silicon), where refraction effects are negligible. The density of electrons per unit of substrate area for the monolayer film, $\rho_{exp}$, is calculated using the obtained electron density profiles according to

$$\rho_{exp} = \int \rho_z(z)\, dz \qquad (5)$$

where integration is taken over the entire film. The molecular footprint can then be calculated from $N_e/\rho_{exp}$, where $N_e$ is the total amount of electrons in a single chromophore. Figure 6 displays normalized reflectivity data ($R/R_F$) from typical scans on films **6**−**10** and shows the best fits (solid lines) using eq 4. Table 2 displays the XRR data.

The films have an electron density, $\rho$, of ∼0.45 e Å$^{-3}$, a thickness of ∼1 nm, and a molecular footprint of ∼50 Å$^2$. The

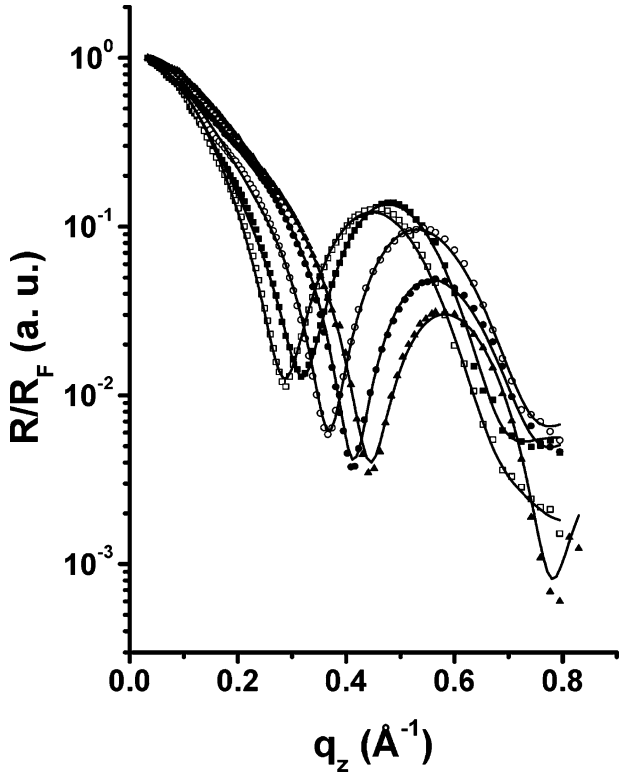


**Figure 6.** Representative normalized synchrotron XRR data for SAMs **6** (■), **7** (□), **8** (●), **9** (○), and **10** (▲). The solid lines are best fits according to eq 4.

XRR-derived film thicknesses are in good agreement with the XPS results for films **7** and **9**. Similar SAMs thickness and electron density values have been reported for related stilbene-, azobenzene- and zwitterionic, and heteroarylethene-based films.[31−34,39,40,42,47,62] The surface roughness, $\sigma_{film-air} \approx 3.2$ Å, is close to that of the Si(100) substrate roughness, $\sigma_{Si-film} \approx 2.3$ Å. Similar values have been reported for highly ordered self-assembled octadecyltrichlorosilane-based films on sili-

**TABLE 2: Structural Parameters of Chromophore Monolayers 6−10 on Si Substrates from the XRR Data**

| film | $\rho_{film}$ (eÅ$^{-3}$) | $\sigma_{Si-film}$ (Å) | $\sigma_{film-air}$ (Å) | $T_{film}$ (nm) | footprint (Å$^2$) |
|---|---|---|---|---|---|
| **6** | 0.45 | 2.1 | 3.2 | 0.9 | 50 |
| **7** | 0.42 | 3.0 | 3.0 | 0.8 | 60 |
| **8** | 0.43 | 2.4 | 3.3 | 1.1 | 48 |
| **9** | 0.44 | 2.5 | 3.4 | 1.2 | 49 |
| **10** | 0.46 | 2.2 | 3.0 | 0.8 | 49 |

con.[58,63−65] From the chromophore layer molecular footprint, the chromophore density ($N_s$) was calculated and is found to be $\sim 2 \times 10^{14}$ molecules/cm$^2$. This value is in accord with previously reported densely packed stilbene- and azobenzene-based monolayers.[31−41,46,47]

## Summary and Conclusions

A series of stilbene-type monolayers were prepared with comparable film thickness, chromophore density, surface morphology, and wettability. The covalently bound monolayers exhibit a relatively high concentration of surface-bound chromophores which are restricted in their orientational freedom. Our observations show that the chromophore−chromophore interactions in fully densified films are a function of the terminal aryl group. The salt-like microstructure of the films does not prevent strong intermolecular $\pi-\pi$ interactions in the naphthalene (**8**) and anthracene (**9**)-based systems. Apparently, molecular aggregation in these systems is not hampered by repulsive electrostatic interactions. It is noteworthy that carbon−carbon double bonds which are polarized by their environment may interact with aromatic rings in adjacent molecules.[66] Our observations show that, by systematic variations of the molecular design of the stilbene building blocks, it is possible to control the in-plane molecular interactions. Specially designed scaffolds, used in other systems,[67] are not necessary here.

## Experimental Section

**Materials and Methods.** Chromophore precursors (**1**−**5**) were synthesized according to published procedures and characterized by $^1$H and $^{13}$C{$^1$H} NMR and UV−vis spectroscopy.[48−51] Reagents were purchased from Aldrich and used as received, unless stated otherwise. Toluene and pentane were dried and degassed using an M. Braun solvent purification system. Tetrahydrofuran (THF) was distilled under $N_2$ from Na and degassed before introduction into an M. Braun glovebox and was stored over activated 4-Å molecular sieves. Deuterated solvents were purchased from Aldrich, degassed, and stored over 4-Å activated molecular sieves in the glovebox. Single-crystal silicon ⟨100⟩ substrates were purchased from Virginia Semiconductor, Inc. Sodium lime glass (Chase Scientific Glass) and silicon substrates ($2.5 \times 2.5$ cm$^2$) were cleaned by immersion in piranha solution [7:3 (v/v) $H_2SO_4$/30% $H_2O_2$] at room temperature for 3 h. (*Caution: piranha solution is an extremely dangerous oxidizing agent and should be handled with care using appropriate personal protection.*) Subsequently, the substrates were rinsed with deionized water followed by the RCA cleaning protocol: 1:5:1 (v/v/v) $NH_3 \cdot H_2O/H_2O/30\%$ $H_2O_2$ at room temperature, 40 min. The substrates were subsequently washed with deionized water and oven-dried (125 °C) overnight. The monolayer formation was carried out under an inert atmosphere using either standard Schlenk/cannula techniques or in an $N_2$-filled M. Braun glovebox with $H_2O$ and $O_2$ levels at <2 ppm. Advancing CAs were measured on a Rame−Hart goniometer. UV−vis spectra were recorded with a Cary 100 spectrophotometer. XRR measurements were carried out with $\lambda = 1.197$ Å on Beam Line X23B of the National Synchrotron Light Source at Brookhaven National Laboratory. Details and the data acquisition and analysis procedures are given elsewhere.[41] XPS measurements were performed on a Kratos Analytical AXIS-HS instrument, using a monochromatized Al Kα source at a power of 75 W and pass energies ranging between 20 and 80 eV. The $^1$H and $^{13}$C{$^1$H} spectra were recorded at 400.19 and 100.6 MHz, respectively, on a Bruker AMX 400 NMR spectrometer and at 250.17 and 62.9 MHz, respectively, on a Bruker DPX 250 NMR spectrometer. All chemical shifts ($\delta$'s) are reported in ppm, and coupling constants ($J$'s) are in Hz. The $^1$H and $^{13}$C{$^1$H} NMR chemical shifts are relative to tetramethylsilane; the resonances of the residual protons of the solvent were used as an internal standard for $^1$H and all-*d* solvent peaks for $^{13}$C. All measurements were carried out at 298 K, unless otherwise stated.

**Formation of Chromophores 6−10.** For **6**: An excess of 3-iodo-*n*-propyl-1-trimethoxysilane (0.741 g, 2.56 mmol) was added to a dry THF solution (20 mL) of chromophore **1** (0.060 g, 0.331 mmol) under $N_2$ in a pressure vessel. The reaction mixture was stirred and heated overnight at 80 °C. Subsequently, the volume was reduced to ~3 mL. The addition of dry pentane (10 mL) at −25°C to the reaction mixture resulted in the precipitation of the desired product. The precipitate was isolated by filtration and dried under high vacuum, yielding chromophore **6** (yield > 90%). Chromophores **7**−**10** were obtained following the same procedure. Concentration-dependent optical (UV−vis) studies with **6**−**10** showed no significant shifts of the charge-transfer bands as a result of chromophore aggregation in solution.

**6**: $^1$H NMR (400 MHz, DMSO-$d_6$) $\delta$ 0.59 (t, $^3J = 8.4$ Hz, 2H; $CH_2Si$), 1.96 (m, 2H; $CH_2$), 3.48 (s, 9H; $Si(OCH_3)_3$), 4.47 (t, $^3J = 8.0$ Hz, 2H; N−$CH_2$), 7.49 (t, $^3J = 8.0$ Hz, 3H; ArH), 7.55 (d, $^3J = 16.4$ Hz, 1H; CH═CH), 7.76 (d, $^3J = 7.0$ Hz, 2H; ArH), 8.04 (d, $^3J = 16.4$ Hz, 1H; CH═CH), 8.26 (d, $^3J = 8.0$ Hz, 2H; pyridine), 8.95 (d, $^3J = 8.0$ Hz, 2H; pyridine). $^{13}$C{$^1$H} NMR (100 MHz, DMSO-$d_6$) $\delta$ 5.79 ($CH_2Si$), 24.86 ($CH_2$), 50.57 ($Si(OCH_3)_3$), 62.21 (N−$CH_2$), 123.8, 124.34 (×2), 128.54 (×2), 129.58 (×2), 130.88, 135.57, 141.21, 144.75 (×2), 153.25. UV−vis (THF) $\lambda$/nm ($\epsilon \times 10^4$) = 219 (2.0), 350 (2.2).

**7**: $^1$H NMR (250 MHz, $CDCl_3$) $\delta$ 0.68 (t, $^3J = 8.3$ Hz, 2H; $CH_2Si$), 2.13 (m, 2H; $CH_2$), 3.56 (s, 9H; $Si(OCH_3)_3$), 4.76 (t, $^3J = 7.3$ Hz, 2H; N−$CH_2$), 7.27 (d, $^3J = 16.4$ Hz, 1H; CH═CH), 7.57 (m, 4H; ArH), 7.77 (d, $^3J = 16.4$ Hz, 1H; CH═CH), 8.17 (d, $^3J = 6.7$ Hz, 2H; pyridine), 9.0 (d, $^3J = 6.8$ Hz, 2H; pyridine). $^{13}$C($^1$H) NMR (62 MHz, acetone-$d_6$) $\delta$ 6.39 ($CH_2Si$), 25.93 ($CH_2$), 50.76 ($Si(OCH_3)_3$), 63.3 (N−$CH_2$), 124.74, 125.0, 125.31 (×2), 130.88 (×2), 133.0 (×2), 135.49, 140.81, 145.31 (×2), 154.41. UV−vis (THF) $\lambda$/nm ($\epsilon \times 10^4$) = 244 (1.9), 353 (3.3).

**8**: $^1$H NMR (400 MHz, $CDCl_3$) $\delta$ 0.66 (t, $^3J = 8.0$ Hz, 2H; $CH_2Si$), 2.08 (m, 2H; $CH_2$), 3.59 (s, 9H; $Si(OCH_3)_3$), 4.67 (t, $^3J = 8.0$ Hz, 2H; N−$CH_2$), 7.24 (d, $^3J = 16.0$ Hz, $^1$H; CH═CH), 7.48 (t, $^3J = 8.0$ Hz, 2H; ArH), 7.59 (t, $^3J = 8.0$ Hz, 1H; ArH), 7.83 (d, $^3J = 8.0$ Hz, 1H; ArH), 7.87 (d, $^3J = 8.0$ Hz, 2H; ArH), 8.18 (d, $^3J = 8.0$ Hz, 2H; pyridine), 8.28 (d, $^3J = 8.0$ Hz, 1H; ArH), 8.46 (d, $^3J = 16.0$ Hz, 1H; CH═CH), 8.99 (d, $^3J = 8.0$ Hz, 2H; pyridine). $^{13}$C{$^1$H} NMR (100 MHz, $CDCl_3$) $\delta$ 6.05 ($CH_2Si$), 25.81 ($CH_2$), 51.22 ($Si(OCH_3)_3$), 62.65 (N−$CH_2$), 123.8, 124.96 (×2), 125.98, 126.85 (×2), 127.74, 129.22, 131.73 (×3), 133.96, 138.87, 144.29, 153.6 (×2). UV−vis (THF) $\lambda$/nm ($\epsilon \times 10^4$) 224 (52.3), 294 (26.6), 368 (13.9).

**9**: $^1$H NMR (400 MHz, $CDCl_3$) $\delta$ 0.74 (t, $^3J$ = 8.0 Hz, 2H; $CH_2Si$), 2.22 (m, 2H; $CH_2$), 3.62 (s, 9H; $Si(OCH_3)_3$), 4.88 (t, $^3J$ = 8.0 Hz, 2H; N—$CH_2$), 7.07 (d, $^3J$ = 16.0 Hz, 1H; CH═CH), 7.54 (m, 4H; ArH), 8.02 (d, $^3J$ = 8.0 Hz, 2H; pyridine), 8.20 (d, $^3J$ = 8.0 Hz, 4H; ArH), 8.47 (1H; ArH), 8.64 (d, $^3J$ = 16.0 Hz, 1H; CH═CH), 9.23 (d, $^3J$ = 8.0 Hz, 2H; pyridine). $^{13}C\{^1H\}$ NMR (100 MHz, $CDCl_3$) $\delta$ 6.08 ($CH_2Si$), 25.89 ($CH_2$), 51.27 ($Si(OCH_3)_3$), 63.03 (N—$CH_2$), 124.67 (×2), 125.15 (×2), 125.96 (×2), 127.46 (×2), 129.05, 129.50 (×2), 129.89, 129.99 (×2), 131.15, 131.58 (×2), 139.84, 144.92, 153.21 (×2). UV−vis (THF) $\lambda$/nm ($\epsilon \times 10^4$) 221 (178.7), 248 (sh), 253 (915.73), 257 (951.69), 292 (296.63), 370 (sh), 459 (66.3).

**10**: $^1$H NMR (400 MHz, acetone-$d_6$) $\delta$ 0.61 (t, $^3J$ = 8.0 Hz, 2H; $CH_2Si$), 2.22 (m, 2H; $CH_2$), 3.57 (s, 9H; $Si(OCH_3)_3$), 4.65 (t, $^3J$ = 8.0 Hz, 2H; N—$CH_2$), 7.34 (d, $^3J$ = 16.0 Hz, 1H; CH═CH), 7.84−9.29 (m, 13H; ArH), 8.66 (d, $^3J$ = 16.0 Hz, 1H; CH═CH). $^{13}C\{^1H\}$ NMR (100 MHz, DMSO-$d_6$) $\delta$ 6.68 ($CH_2Si$), 25.86 ($CH_2$), 51.24 ($Si(OCH_3)_3$), 63.14, 124.32, 125.42, 125.6 (×2), 126.64, 126.93, 127.18, 127.46, 127.9 (×2), 128.58 (×2), 129.78, 129.98, 130.30, 131.62, 132.24 (×2), 133.68, 138.3, 145.5 (×2), 153.21. UV−vis (THF) $\lambda$/nm ($\epsilon \times 10^4$) 275 (5.09), 295 (5.09), 321 (4.73), 341 (sh), 394 (3.82), 447 (4.36).

**Monolayer Formation.** Under $N_2$, freshly cleaned sodium lime glass, and/or silicon substrates were loaded into a Teflon sample holder and immersed in dry THF solutions (1.0 mM) of chromophores **6**−**10** and heated at 70 °C for 24 h in a sealed pressure vessel with the exclusion of light. The functionalized substrates were then rinsed with THF, acetone, and 2-propanol and sonicated in THF for 3 min. The substrates were dried under a stream of $N_2$ and stored under $N_2$ with the exclusion of light. The assembly process can be carried out in a single reaction vessel using standard cannula techniques to transfer the solutions; however, most experiments were performed in a glovebox.

**Follow-Up of Monolayer Formation.** The freshly cleaned sodium lime glass substrates were fixed in a Telfon sample holder and fully immersed in a toluene solution (1.0 mM) of **9**. The airtight reaction vessels were fully immersed in a temperature-controlled oil bath at 60 ± 2 °C. Film growth was quenched after measured time intervals ($t$ = 20 min, 1 h, and 16 h). The substrates (2.5 × 2.5 cm$^2$) were immediately washed with excess dry toluene and THF, sonicated in acetone for 2 min., and then dried at room temperature under a flow of $N_2$. Similar procedures were used for **8** and **10**.

**Acknowledgment.** X-ray reflectivity measurements were performed at Beam Line X23B of the National Synchrotron Light Source, which is supported by the U.S. Department of Energy. This research was supported by the Robert Rees Fund for Applied Research, the MJRG for Molecular Materials and Interface Design, BMBF, MINERVA, and by the Yigal-Alon Fellowship program (M.E.vd.B.). We thank Dr. Y. Feldman (WIS) for the AFM measurements. A.D.S. is the recipient of The Reva G. Stone Postdoctoral Fellowship. M.E.vd.B. is the incumbent of the Dewey David Stone and Harry Levine career development chair. A.D. thanks DST (India) for financial assistance.

## References and Notes

(1) Shi, Y.; Zhang, C.; Zhang, H.; Bechtel, J. H.; Dalton, L. R.; Robinson, B. H.; Steier, W. H. *Science* **2000**, *288*, 119.

(2) Ma, H.; Chen, B.; Sassa, T.; Dalton, L. R.; Jen, A. K.-Y. *J. Am. Chem. Soc.* **2001**, *123*, 986.

(3) van der Boom, M. E. *Angew. Chem., Int. Ed.* **2002**, *41*, 3363.

(4) Mas-Torrent, M.; Durkut, M.; Hadley, P.; Ribas, X.; Rovira, C. *J. Am. Chem. Soc.* **2004**, *126*, 984.

(5) Meijer, E. J.; De Leeuw, D. M.; Setayesh, S.; van Veenendaal, E.; Huisman, B.-H.; Blom, P. W. M.; Hummelen, J. C.; Scherf, U.; Klapwijk, T. M. *Nat.ure Mater.* **2003**, *2*, 678.

(6) Mushrush, M.; Facchetti, A.; Lefenfeld, M.; Katz, H. E.; Marks, T. J. *J. Am. Chem. Soc.* **2003**, *125*, 9414.

(7) Würthner, F.; Wortmann, R.; Meerholz, K. *ChemPhysChem* **2002**, *3*, 17.

(8) Sautter, A.; Thalacker, C.; Heise, B.; Wurthner, F. *Proc. Natl. Acad. Sci. U.S.A.* **2002**, *99*, 4993.

(9) Dalton, L. R.; Harper, A. W.; Robinson, B. H. *Proc. Natl. Acad. Sci. U.S.A.* **1997**, *94*, 4842.

(10) Dela Cruz, J. L.; Blanchard, G. J. *J. Phys. Chem. A* **2002**, *106*, 10718.

(11) Horne, J. C.; Blanchard, G. J. *J. Am. Chem. Soc.* **1999**, *121*, 4427.

(12) Ricceri, R.; Neto, C.; Abbotto, A.; Facchetti, A.; Pagani, G. A. *Langmuir* **1999**, *15*, 2149.

(13) Ricceri, R.; Grando, D.; Abbotto, A.; Facchetti, A.; Pagani, G. A.; Gabrielli, G. *Langmuir* **1997**, *13*, 5787.

(14) Ricceri, R.; Abbotto, A.; Facchetti, A.; Pagani, G. A.; Gabrielli, G. *Thin Solid Films* **1999**, *340*, 218.

(15) van der Boom, T.; Hayes, R. T.; Zhao, Y.; Bushard, P. J.; Weiss, E. A.; Wasielewski, M. R. *J. Am. Chem. Soc.* **2002**, *124*, 9582.

(16) Nguyen, T.-Q.; Martel, R.; Avouris, P.; Bushey, M. L.; Brus, L.; Nuckolls, C. *J. Am. Chem. Soc.* **2004**, *126*, 5234-5242.

(17) Yerushalmi, R.; Scherz, A.; van der Boom, M. E. *J. Am. Chem. Soc.* **2004**, *126*, 2700.

(18) Lundquist, P. M.; Yitzchaik, S.; Marks, T. J.; Wong, G.; Di Bella, S.; Cohen, R.; Berkovic, G. *Phys. Rev. B* **1997**, *55*, 14055.

(19) Reyes-Esqueda, J.; Darracq, B.; Garcia-Macedo, J.; Canva, M.; Blanchard-Desce, M.; Chaput, F.; Lahil, K.; Boilot, J. P.; Brun, A.; Levy, Y. *Opt. Commun.* **2001**, *198*, 207.

(20) Shoji, O.; Higashi, Y.; Hishinuma, S.; Sato, M.; Annaka, M.; Yoshikuni, M.; Nakahira, T. *Macromolecules* **2002**, *35*, 2116.

(21) Würthner, F.; Yao, S. *Angew. Chem., Int. Ed.* **2000**, *39*, 1243.

(22) Angelova, A.; Ionov, R. *Langmuir* **1999**, *51*, 7199.

(23) Matsumoto, M.; Nakazawa, T.; Mallia, V. A.; Tamaoki, N.; Azumi, R.; Sakai, H.; Abe, M. *J. Am. Chem. Soc.* **2004**, *126*, 1006.

(24) Vranken, N.; Foubert, P.; Koehn, F.; Gronheid, R.; Scheblykin, I.; Van der Auweraer, M.; De Schryver, F. C. *Langmuir* **2002**, *18*, 8407.

(25) Li, F.-Y.; Huang, C.-H.; Jin, L.-P.; Wu, D.-G.; Zhao, X.-S. *J. Mater. Chem.* **2001**, *11*, 3002.

(26) Farahat, C. W.; Penner, T. L.; Ulman, A.; Whitten, D. G. *J. Phys. Chem.* **1996**, *100*, 12616.

(27) Di Bella, S.; Lanza, G.; Fragalà, I.; Yitzchaik, S.; Ratner, M. A.; Marks, T. J. *J. Am. Chem. Soc.* **1997**, *119*, 3003.

(28) Yitzchaik, S.; Di Bella, S.; Lundquist, P. M.; Wong, G. K.; Marks, T. J. *J. Am. Chem. Soc.* **1997**, *119*, 2995.

(29) Di Bella, S.; Fragala, I.; Marks, T. J. *Isr. J. Chem.* **2000**, *40*, 123.

(30) von Berlepsch, H.; Böttcher, C.; Ouart, A.; Burger, C.; Dähne, S.; Kirstein, S. *J. Phys. Chem. B* **2000**, *104*, 5255.

(31) Li, D.; Ratner, M.; Marks, T. J.; Zhang, C.; Yang, J.; Wong, G. *J. Am. Chem. Soc.* **1990**, *112*, 7389.

(32) van der Boom, M. E.; Evmenenko, G.; Dutta, P.; Marks, T. J. *Adv. Funct. Mater.* **2001**, *11*, 393.

(33) van der Boom, M. E.; Richter, A. G.; Malinsky, J. E.; Lee, P.; Armstrong, N. R.; Dutta, P.; Marks, T. J. *Chem. Mater.* **2001**, *13*, 15.

(34) van der Boom, M. E.; Zhu, P.; Evmenenko, G.; Malinsky, J. E.; Lin, W.; Dutta, P.; Marks, T. J. *Langmuir* **2002**, *18*, 3704.

(35) Zhu, P.; van der Boom, M. E.; Kang, H.; Evmenenko, G.; Dutta, P.; Marks, T. J. *Chem. Mater.* **2002**, *14*, 4982.

(36) Facchetti, A.; van der Boom, M. E.; Abbotto, A.; Beverina, L.; Marks, T. J.; Pagani, G. A. *Langmuir* **2001**, *17*, 5939.

(37) Facchetti, A.; Abbotto, A.; Beverina, L.; van der Boom, M. E.; Dutta, P.; Evmenenko, G.; Marks, T. J.; Pagani, G. A. *Chem. Mater.* **2002**, *14*, 4996.

(38) Facchetti, A.; Abbotto, A.; Beverina, L.; van der Boom, M. E.; Marks, T. J.; Pagani, G. A. *Chem. Mater.* **2002**, *14*, 4996.

(39) Lin, W.; Lin, W.; Wong, G. K.; Marks, T. J. *J. Am. Chem. Soc.* **1996**, *118*, 8034.

(40) Yitzchaik, S.; Marks, T. J. *Acc. Chem. Res.* **1996**, *29*, 197.

(41) Evmenenko, G.; van der Boom, M. E.; Kmetko, J.; Dugan, S. W.; Marks, T. J.; Dutta, P. *J. Chem. Phys.* **2001**, *115*, 6722.

(42) van der Boom, M. E.; Malinsky, J. E.; Zhao, C.-F.; Chang, S.; Lu, W.-K.; Ho, S. T.; Marks, T. J. *Polym. Prepr. (Am. Chem. Soc., Div. Polym. Chem.)* **2001**, *42*, 550−551.

(43) Zhao, Y. G.; Wu, A.; Lu, H. L.; Chang, S.; Lu, W. K.; Ho, S. T.; van der Boom, M. E. *Appl. Phys. Lett.* **2001**, *79*, 587.

(44) Zhao, Y. G.; Chang, S.; Wu, A.; Lu, H. L.; Ho, S. T.; van der Boom, M. E.; Marks, T. J. *Opt. Eng. Lett.* **2003**, *42*, 298.

(45) Lundquist, P. M.; Lin, W.; Zhou, H.; Hahn, D. N.; Yitzchaik, S.; Marks, T. J.; Wong, G. K. *Appl. Phys. Lett.* **1997**, *70*, 1941.

(46) Yitzchaik, S.; Roscoe, S. B.; Kakkar, A. K.; Allan, D. S.; Marks, T. J.; Xu, Z.; Zhang, T.; Lin, W.; Wong, G. K. *J. Phys. Chem.* **1993**, *97*, 6958.

(47) van der Boom, M. E.; Evmenenko, G.; Yu, C.-J.; Pulak, D.; Marks, T. J. *Langmuir* **2003**, *19*, 10531.

(48) Williams, J. L. R.; Adel, R. E.; Carlson, J. M.; Reynolds, G. A.; Borden, D. G.; Ford, J. A. *J. Org. Chem.* **1963**, *28*, 387.

(49) Burdeniuk, J.; Milstein, D. *J. Organomet. Chem.* **1993**, *451*, 213.

(50) Sankaran, N. B.; Das, A.; Samanta, A. *Chem. Phys. Lett.* **2002**, *351*, 61.

(51) Vernigor, E. M.; Koz'menko, M. V.; Lebedev, S. A.; Luk'yanets, E. A.; Savvina, L. P.; Shalaev, V. K. *Khim. Geterotsikl. Soedin.* **1987**, *6*, 820.

(52) Kasha, M. *Radiat. Res.* **1963**, *20*, 55.

(53) Khairutdinov, R. F.; Serpone, N. *J. Phys Chem. B* **1999**, *103*, 761.

(54) Bierbaum, K.; Grunze, M.; Baski, A. A.; Chi, L. F.; Schrepp, W.; Fuchs, H. *Langmuir* **1995**, *11*, 2143.

(55) Schwartz, D. K.; Steinberg, S.; Israelachvili, J. N.; Zasadzinski, J. A. N. *Phys. Rev. Lett.* **1992**, *69*, 3354.

(56) Angst, D. L.; Simmons, G. W. *Langmuir* **1991**, *7*, 2236.

(57) Tidswell, I. M.; Ocko, B. M.; Pershan, P. S.; Wasserman, S. R.; Whitesides, G. M.; Axe, J. D. *Phys. Rev. B* **1990**, *41*, 1111.

(58) Wasserman, S. R.; Tao, Y.-T.; Whitesides, G. M. *Langmuir* **1989**, *5*, 1074.

(59) Richter, A. G.; Yu, C.-J.; Datta, A.; Kmetko, J.; Dutta, P. *Phys. Rev. E* **2000**, *61*, 607.

(60) Carraro, C.; Yauw, O. W.; Sung, M. M.; Maboudian, R. *J. Phys. Chem. B* **1998**, *102*, 4441.

(61) The films were found to be reasonably stable against prolonged X-ray irradiation. In time, some film damage occurs, as evident from the appearance of several additional N signals in both **7** and **9**, and decreasing of the Br signals (71.78, 70.75 eV) for film **7**.

(62) van der Boom, M. E.; Richter, A. G.; Malinsky, J. E.; Pulak, D.; Marks, T. J.; Lee, P. A.; Armstrong, N. R. *Polym. Mater. Sci. Eng.* **2000**, *83*, 160.

(63) Bierbaum, K.; Kinzler, M.; Wöll, Ch.; Grunze, M.; Hahner, G.; Heid, S.; Effenberger, F. *Langmuir* **1995**, *11*, 512.

(64) Ohtake, T.; Mino, N.; Ogana, K. *Langmuir* **1992**, *8*, 2081.

(65) Pomerantz, M.; Segmüller, A.; Netzer, L.; Sagiv, J. *Thin Solid Films* **1985**, *132*, 153.

(66) Hanson, A. W. *Acta Crystallogr.* **1965**, *19*, 610.

(67) van der Boom, T.; Evmenenko, G.; Dutta, P.; Wasielewski, M. R. *Chem. Mater.* **2003**, *15*, 4068.